

# Robustness of spatial-coherence multiplexing under receiver misalignment

Lawrence J. Pelz and Betty Lise Anderson

It has been shown previously that the spatial coherence of a source can be modulated and demodulated; hence it can be used as the basis for a new dimension of multiplexing in high-speed optical communication links. We address the sensitivity of such a system to misalignments of the receiver with respect to the beam and examine how changing transverse modes affect the spatial coherence in the lateral direction. Specifically, we show that such a system is surprisingly robust for both lateral offsets, in which the receiver is not properly aligned on the beam center, and rotational offsets, in which the receiver is tilted with respect to the plane of the spatial coherence modulation. The presence of higher-order transverse modes or changes in the transverse-mode structure are also shown to have little effect on the system operation. © 1998 Optical Society of America

*OCIS codes:* 030.1640, 060.4230, 030.4070.

## 1. Introduction

There is always a need for increased speed and capacity for optical communication links. One approach to increasing link capacity is to superimpose various orthogonal types of multiplexing, for example, combining intensity modulation with wavelength-division multiplexing to use the full capacity of a channel. Photonic systems can also use polarization and coherence multiplexing. Coherence multiplexing can use temporal coherence,<sup>1-4</sup> and recently a scheme for exploiting the spatial coherence was proposed.<sup>5</sup> The spatial coherence is modulated by varying of the spatial modes of a light source.

In this paper we examine the effects of receiver misalignment on the reliability of a spatial-coherence multiplexed link, as well as the effect of any unwanted or changing modes in the direction perpendicular to that of the modulation. For misalignment the effect of lateral offset of the receiver with respect to the beam center is examined, as well as the impact of rotation of the receiver input plane with respect to the transmitter's modulation plane. Then we study the effects of the existence of higher-order modes in a

direction perpendicular to the direction of interest: For example, if the  $x$ -dependent (lateral) modes are the ones that are modulated, what is the impact if the  $y$ -dependent (transverse) modes are also changed?

We begin with a brief summary of the spatial-coherence modulation technique in Section 2. The attending theory is reviewed in Section 3. In Sections 4 and 5 we address the effects of lateral and rotational offsets. In Section 6 we discuss the effects of the higher-order transverse modes. We summarize our conclusions in Section 7.

## 2. Spatial-Coherence Modulation

The spatial-coherence properties of a laser beam are determined directly by the transverse-mode structure composing that beam. To see the effect of the spatial-mode structure on the spatial coherence of a light beam, consider a laser or waveguide carrying monochromatic light emitting in a single spatial mode. There is unity (perfect) spatial coherence everywhere across the beam. When one or more higher-order spatial modes are also present, the spatial-coherence function (SCF) exhibits maxima and minima at predictable locations.<sup>6,7</sup>

The effect of the spatial modes on the spatial coherence can be exploited. It follows that, by intentionally modulating the spatial-mode structure of a source, one can also modulate the SCF. A spatial-mode modulator was proposed to perform this function. Information encoded onto the spatial-coherence state of the beam is demodulated with a simple interferometer.<sup>5</sup>

The transmitter or modulator was taken in Ref. 5

---

The authors are with the Department of Electrical Engineering, Ohio State University, 205 Dreese Laboratory, 2015 Neil Avenue, Columbus, Ohio 43210.

Received 2 January 1997; revised manuscript received 13 June 1997.

0003-6935/98/050815-06\$10.00/0

© 1998 Optical Society of America

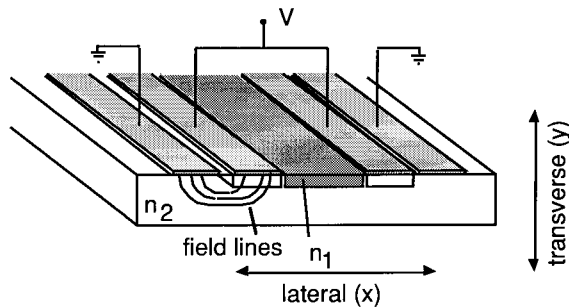


Fig. 1. Electro-optic modulator used to change the number of spatial modes of a beam.

to be an electro-optic waveguiding device. In one configuration a single passive waveguide is flanked on either side by adjacent electro-optically controlled waveguides, as shown in Fig. 1. When no voltage is applied, the light effectively reaches only the center passive waveguide, which supports a single spatial mode. When the outrigger waveguides are activated, their refractive indices change to match that of the passive central waveguide, making the effective waveguide wider and able to support the next higher-order mode.

One measures the spatial coherence by interfering the electric fields at two points on the beam  $(x, -x)$  chosen symmetrically about the beam center. The visibility of the interference fringes is a direct measure of the spatial coherence  $|\mu|$  if the beam is symmetric.<sup>8</sup> Figure 2 shows the calculated effect of the changing spatial modes on the SCF.<sup>6</sup> When a single spatial mode is present, the spatial coherence is unity everywhere, i.e., the interferometer would produce high-visibility fringes. When the next-higher-order mode is present as well, the SCF goes to zero at some particular value of  $\pm x$ . The plot shows this point as a function of the spot size  $\sigma$ , which is the  $1/e^2$  intensity point of the fundamental mode. The location of that zero is determined uniquely by the proportion of the total energy carried in each of the spatial modes.

The receiver therefore is an interferometer that is designed to combine the fields from the particular  $\pm x$

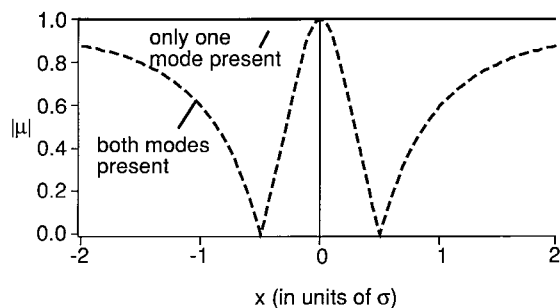


Fig. 2. SCF  $|\mu(x, -x)|$  as a function of  $x$ , the distance from the beam center. Solid line: Only one spatial mode is present. Dashed curve: Two modes are present in equal weights. The spot size  $\sigma$  is measured at the  $1/e^2$  intensity point of the fundamental mode.

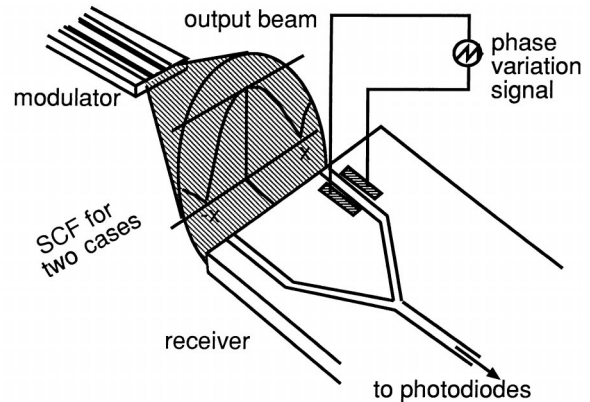


Fig. 3. Electro-optic demodulator device as an interferometer that measures the visibility corresponding to the SCF  $|\mu(x, -x)|$ .

at which the SCF will go to zero. As mentioned above, that location depends on the modal weights. It has been shown that a 50:50 ratio of the fundamental to the first higher-order lateral mode is optimum for communication purposes because, at the locations of zeros of the SCF for this particular modal distribution, the intensity of the beam does not change whether there is one mode or two present.<sup>5</sup> An electro-optic SCF demodulator or receiver is shown in Fig. 3. The receiver is a waveguide version of Young's classical two-pinhole interferometer.<sup>9</sup> The two arms sample the beam at  $\pm x$ . For measuring the spatial coherence some optical path difference must be introduced to produce constructive and destructive interference. One can accomplish this by electro-optically varying the refractive index of one arm. As one beam is delayed with respect to the other, the interferometer output intensity goes through minima and maxima. We refer to these peaks and valleys as fringes, although they are not manifested in space but rather in time, as a function of the applied voltage. The amplitude of the fringes directly measures the state of coherence, whereas the intensity of the beam remains unchanged.

Operation of the link is as follows: When the modulator is OFF, that is, no voltage is applied, the waveguide supports a single spatial (let us say, lat-

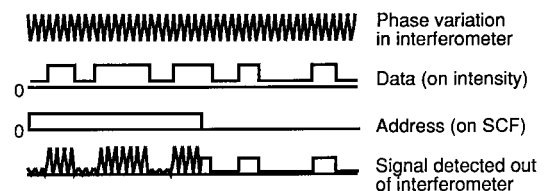


Fig. 4. Signals of a spatial-coherence-multiplexed link. The voltage applied to the receiver increases linearly, so that fringes (top signal) appear at the receiver output when there is coherence (first half of SCF signal). The intensity varies from high to low (not zero), as shown in the second line of the figure. The resulting detected signal shows bright and dim fringes when the SCF equals 1, and it shows bright and dim light with no fringes when the SCF equals zero.

eral) mode. The beam is incident on the receiver, which samples it at  $\pm x$ . The fields at  $\pm x$  propagate through the interferometer and are combined at the detector. A ramp voltage is applied to one arm, however, so the refractive index of the material in that arm changes linearly, thus introducing a phase delay for that part of the field. The frequency of the fringes is determined by the slope of the ramp and the electro-optic coefficient, and it can thus be extremely fast.

When voltage is applied to the modulator, two lateral modes are supported, the SCF goes to zero at  $(x, -x)$ , and no fringes are observed at the detector since there is no longer any coherence between the fields at these two points. Examples of the signals of a spatial-coherence multiplexed link are shown in

point  $(x, y)$ , which is the sum of the fields of each of the modes, in the form

$$E(x, y, t) = \sum_n \sum_m a_n a_m f_n(x) f_m(y) \times \exp\{i[\omega t + \phi_n(t) + \phi_m(t)]\}, \quad (1)$$

where  $a_{n,m}$  is the amplitude of the  $n$ th  $x$ -dependent and  $m$ th  $y$ -dependent mode,  $f_n(x)$  is the functional form of the  $n$ th lateral mode,  $f_m(y)$  is the functional form of the  $m$ th transverse mode,  $\omega$  is the central angular frequency, and  $\phi_{n,m}(t)$  are the phase dependencies. In general, there will be a time delay  $\tau$  between the fields arriving from the two arms of the interferometer. The total intensity measured at the detector is

$$\begin{aligned} I(\mathbf{r}_1, \mathbf{r}_2) &= \langle [E(x_1, y_1, t) + E(x_2, y_2, t + \tau)] * [E(x_1, y_1, t) + E(x_2, y_2, t + \tau)] \rangle \\ &= \left\langle \left( \begin{array}{l} \sum_n \sum_m a_n a_m f_n(x_1) f_m(y_1) \exp\{i[\omega t + \phi_n(t) + \phi_m(t)]\} \\ \sum_n \sum_m a_n a_m f_n(x_2) f_m(y_2) \exp\{i[\omega(t + \tau) + \phi_n(t + \tau) + \phi_m(t + \tau)]\} \end{array} \right) \text{c.c.} \right\rangle \\ &= \sum_n \sum_m a_n^2 a_m^2 f_n^2(x_1) f_m^2(y_1) + \sum_n \sum_m a_n^2 a_m^2 f_n^2(x_2) f_m^2(y_2) \\ &\quad + 2 \operatorname{Re} \left[ \sum_n \sum_m a_n^2 a_m^2 f_n(x_1) f_n(x_2) f_m(y_1) f_m(y_2) \exp(i\omega\tau) \right], \end{aligned} \quad (2)$$

Fig. 4. We assume that the modal weights have been chosen properly such that the intensities at the points  $\pm x$  do not change. Therefore the intensity can additionally be modulated independently of the spatial coherence. In this way an extra degree of multiplexing is achieved. For example, as shown in Fig. 4, data could be modulated onto the intensity and address information could be encoded onto the spatial-coherence state.

For information carried on the beam intensity to be distinguished completely from information carried on the spatial coherence, the two arms of the receiver interferometer must be at exactly the correct locations  $(x, -x)$ . If the receiver is misaligned, cross talk will occur. The sensitivity of such a system to various types of misalignment is the subject of this paper. We begin in Section 3 by reviewing briefly the equations governing this system; then in the subsequent sections we perturb those equations to allow for misalignment.

### 3. Brief Review of the Theory

The relation between spatial coherence and the spatial modes has been developed in Ref. 6, and expressions for predicting the locations of the zeros are given in Ref. 7. Using the coordinate system shown in Fig. 1, let us write the total electric field at some

where  $\mathbf{r}_1$  and  $\mathbf{r}_2$  represent points  $(x_1, y_1)$  and  $(x_2, y_2)$ , respectively. In the last step we assumed the time averaging to be over a sufficiently long time so that terms of the form  $\phi_n(t) - \phi_n(t - \tau)$  average to zero. The first two terms in the last line of Eq. (2) are the intensities in arms 1 and 2, respectively, of the interferometer. The last term can be written in the form<sup>8</sup>

$$2\sqrt{I_1 I_2} |\mu(\mathbf{r}_1, \mathbf{r}_2)| \cos(\omega\tau), \quad (3)$$

where  $I_1$  and  $I_2$  are the intensities at  $\mathbf{r}_1$  and  $\mathbf{r}_2$  and  $\mu$  is the magnitude of the complex degree of spatial coherence. The cosine function is the origin of the fringes that appear as the time delay  $\tau$  is varied, while the amplitude of these fringes depends on  $|\mu|$ .

Assuming the fields are symmetric about the beam center, we can then define the magnitude of the degree of spatial coherence as

$$\begin{aligned} |\mu(\mathbf{r}_1, \mathbf{r}_2)| &= \frac{\sum_n \sum_m a_n^2 a_m^2 f_n(x_1) f_n(x_2) f_m(y_1) f_m(y_2)}{\left[ \sum_n \sum_m a_n^2 a_m^2 f_n^2(x_1) f_m^2(y_1) \sum_n \sum_m a_n^2 a_m^2 f_n^2(x_2) f_m^2(y_2) \right]^{1/2}}. \end{aligned} \quad (4)$$

The detection circuitry will not measure the state of spatial coherence directly but rather will measure

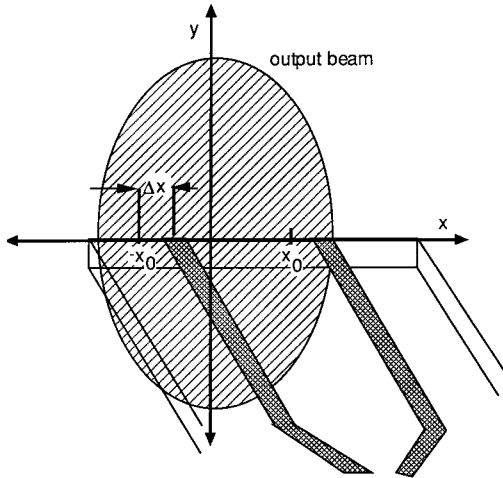


Fig. 5. Geometry for lateral misalignment of the receiver.

the strength of the signal at the fringe frequency. When the coherence is high the amplitude of the fringes is high, and when the coherence is zero the energy at the fringe frequency is zero, even though there is light present. By measuring the fringe amplitudes relative to the total power, the receiver in effect measures the fringe visibility  $V$ , given by

$$V = \frac{I_{\max} - I_{\min}}{I_{\max} + I_{\min}} = \frac{2\sqrt{I_1(\mathbf{r}_1)}\sqrt{I_2(\mathbf{r}_2)}}{I_1(\mathbf{r}_1) + I_2(\mathbf{r}_2)} |\mu(\mathbf{r}_1, \mathbf{r}_2)|. \quad (5)$$

#### 4. Effects of Translational Offset

The receiver can be offset from the beam center owing to a translational misalignment. We assume for this discussion that the modal structure under modulation is the lateral direction; the transverse modes, whatever they are, do not change. The receiver interferometer arms are in the  $x$ - $z$  plane.

First, consider a translational offset of the receiver in the  $y$  direction only, such that the sampling points are  $(x_1, y_1)$  and  $(-x_1, y_1)$  instead of  $(x_1, 0)$  and  $(-x_1, 0)$ . For these sampling points the spatial coherence given in Eq. (4) becomes

$$\begin{aligned} & |\mu(x_1, y_1; -x_1, y_1)| \\ &= \frac{\sum_n a_n^2 f_n(x_1) f_n(-x_1) \sum_m a_m^2 f_m^2(y_1)}{\left[ \sum_n a_n^2 f_n^2(x_1) \right]^{1/2} \left[ \sum_n a_n^2 f_n^2(-x_1) \right]^{1/2} \sum_m a_m^2 f_m^2(y_1)} \\ &= \frac{\sum_n a_n^2 f_n(x_1) f_n(-x_1)}{\left[ \sum_n a_n^2 f_n^2(x_1) \right]^{1/2} \left[ \sum_n a_n^2 f_n^2(-x_1) \right]^{1/2}}. \quad (6) \end{aligned}$$

In other words, the spatial coherence in the  $x$  direction is independent of the choice of  $y$ . This result follows directly from the assumption that the  $x$  and  $y$  dependencies are separable, as is the case, for example, with Hermite-Gaussian modes. This result confers the advantage that several interferometers of

different arm spacings can be stacked in the  $y$  direction, and each looks for zeros in the  $x$  direction at different places on the same beam. In other words, they look for different modal weights for the coding of complex addresses.<sup>5</sup>

For offsets in the  $x$  direction, as shown in Fig. 5, we evaluate Eq. (4) at the points  $(x_0 + \Delta x, y_0)$ ,  $(-x_0 + \Delta x, y_0)$  for the two cases of interest: a single lateral mode and two lateral modes of equal modal weight. When there is a single lateral mode Eq. (4) tells us there is no difference in the spatial coherence; it is unity for any two sampling points  $(x_1, x_2)$ . However, the visibility of the fringes *does* change, according to Eq. (5), because the intensities at the two interferometer arms are not equal when they are offset laterally from the beam center. Figure 6(a) shows the coherence and the visibility for the single-mode case (call it a logic 1) as a function of lateral misalignment in units of  $\sigma$ , the intensity's  $1/e^2$  beam radius, and the assumption of Hermite-Gaussian modes. For the two-mode case the spatial coherence and the visibility are shown in Fig. 6(b). The visibility reaches a maximum and then decreases again with increasing misalignment, even though the coherence constantly increases. This is due to the fact that the intensities at the two interferometer arms differ increasingly from each other as the receiver is increasingly misaligned laterally.

The extinction ratio  $\epsilon$  can be defined as the signal strength of a logic 0 divided by the signal strength of a logic 1. Here the signal is the visibility, and the extinction ratio is

$$\epsilon = \frac{V_0}{V_1}, \quad (7)$$

where  $V_0$  and  $V_1$  are the visibilities of the fringes for the logic 0 and logic 1 cases, respectively. For an ideally aligned system the extinction ratio is 0. Figure 6(c) shows the change in extinction ratio as a function of lateral offset,  $\Delta x$ . The extinction ratio usually varies between 0 and 1, but here it is possible for the signal strength of a logic 0 to exceed the signal strength of a logic 1. That is, for some lateral offsets the visibility of the fringes for the two-mode case actually exceeds the visibility for the one-mode case, a clearly undesirable result. If we set an extinction ratio of 0.1 as an arbitrary tolerable limit, the lateral offset can be up to 0.21  $\sigma$ , or 21% of the beam radius.

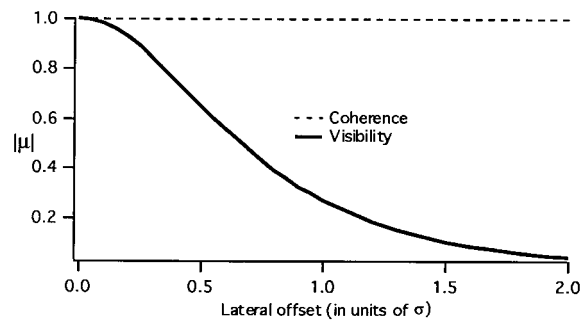
#### 5. Effects of Rotational Misalignment

The geometry of the rotational misalignment is shown in Fig. 7. Here we address the question of what happens when the interferometer arms do not lie precisely in the  $x$ - $z$  plane. If the rotation angle is  $\theta$ , the intended measurement points  $(\pm x_1, 0)$  become  $(+x_2, +y_2)$  and  $(-x_2, -y_2)$ , where

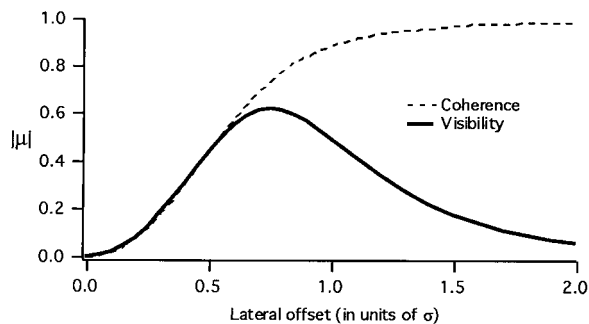
$$x_2 = x_1 \cos \theta, \quad (8)$$

$$y_2 = x_1 \sin \theta. \quad (9)$$

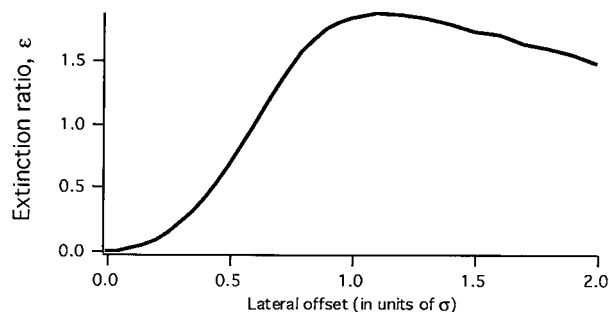
In this case the problem becomes more complicated, since we must take into account the  $y$  variation in the field as well as the  $x$ .



(a)



(b)



(c)

Fig. 6. Effect of lateral offsets on the spatial coherence and visibility (a) when one lateral mode is present and (b) when two lateral modes are present in equal weights. (c) The resulting extinction ratio. The extinction ratio exceeds 1 for some misalignments because the visibility for logic 0 can exceed the visibility for logic 1 for some misalignments.

Unlike the case of translational offset, rotation has no effect on the measured visibility, since under rotation the sampling points are still symmetric about the beam center. For the single lateral-mode case, the visibility remains unity at all angles of misalignment. For the case when two lateral modes are present, as usual in equal weights, the coherence and visibility do change. Figure 8 shows the resulting change in extinction ratio as a function of rotational misalignment, again assuming Hermite–Gaussian modes. We assume there is always a single transverse mode. At  $10^\circ$  of tilt the extinction ratio is approximately 0.01, and it does not reach 0.1, our arbitrary limit of acceptability, until the tilt angle is  $27^\circ$ , a very serious misalignment indeed.

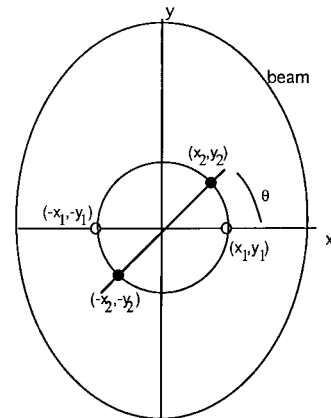


Fig. 7. Rotational misalignment geometry. Open circles indicate the locations of intended measurements; filled circles indicate the actual measurement locations.

## 6. Effect of Higher-Order Transverse Modes

Because the modulator device is likely to be less than ideal, we should consider the possibility that, when the voltage is applied to permit higher-order lateral modes, the waveguide may also support some small amount of energy in a higher-order transverse ( $y$ ) mode.

We assume, as usual, Hermite–Gaussian modes. We are expecting to modulate the source beam between the two states: (1) all energy in  $TEM_{00}$  and (2) energy equally divided between  $TEM_{00}$  and  $TEM_{10}$ . If we assume that the energy is equal in the two lateral modes (for the second state) but that some energy is also now present in  $TEM_{01}$ , what is the effect on the communication link?

We have already shown in Section 4 that the spatial coherence, when measured in the  $x$  direction, is independent of the modal structure in the  $y$  direction. This is true whether or not there is a lateral offset. Under rotation misalignment, however, the transverse modes start to play a role. Figure 9 shows the changing SCF in the neighborhood of one of the zeros as the strength of the  $TEM_{01}$  mode is increased, keeping  $TEM_{00}$  and  $TEM_{10}$  in equal strengths. The curves are plotted for an angular misalignment of  $10^\circ$ . The left-most curve is for the case in which there is no energy in the higher-order transverse mode, and the subsequent curves to the right are for 10%, 20%, 30%,

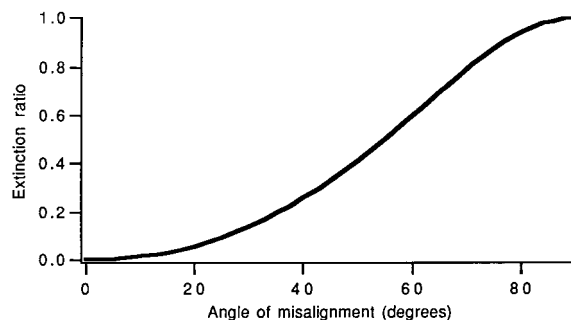


Fig. 8. Effect of tilt misalignment on the extinction ratio.

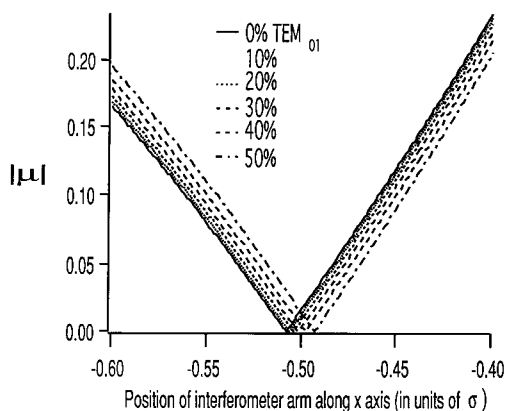


Fig. 9. Close-up of the effect of higher-order transverse ( $y$ -dependent) modes on one of the SCF zeros. The tilt angle is  $10^\circ$ ; the strengths of the  $TEM_{00}$  and  $TEM_{10}$  modes are equal in all cases. The left-most curve is for the case in which none of the energy is in the  $TEM_{01}$  mode.

40%, and 50%, respectively, of the total beam energy that is present in  $TEM_{01}$ . If the interferometer arms are set at  $\pm x = 0.5\sigma$ , where the SCF zero is expected for the ideal case, then the measured fringe visibility will change from the expected value of  $V = 0$  to only  $V = 0.02$ , even when as much as 50% of the total beam energy is in a higher-order transverse instead of the lateral mode. It is also interesting to note that, if the weights in  $TEM_{00}$ ,  $TEM_{10}$ , and  $TEM_{01}$  are all equal (33% of the energy in each), then the spatial coherence is invariant with the rotation angle.

## 7. Summary and Conclusions

We have examined the robustness of a proposed communication link based on modulating the spatial-mode structure and therefore the spatial coherence of a laser beam. The modulator is a waveguide that is electro-optically controlled to support either one lateral mode (spatial coherence is unity) or two lateral modes (spatial coherence is zero at certain positions on the beam). The state of coherence is detected by an electro-optic interferometer that produces extremely high-speed fringes (temporal fringes, not spatial ones) when the modulator is in one state and no fringes in the other state. The coherence is independent of the light intensity for properly chosen operating conditions, so the spatial coherence can be modulated independently of the intensity and thus a single beam can be made to carry two signals instead of one.

We have shown the link to be completely insensitive to transverse misalignments when the modes that are modulated are in the lateral direction. For lateral offsets, that is, in the same plane as the modulation, there is a degradation of the extinction ratio. If we set  $\epsilon = 0.10$  as an upper limit of acceptability, the system can tolerate a lateral displacement of the interferometer arms of up to 21% of the  $1/e^2$  beam-spot size  $\sigma$ . If the interferometer was rotated rather than translated, we found that, with the same upper

limit of 0.1 for the extinction ratio, the rotation can be as much as  $27^\circ$  from the correct plane.

Finally, if higher-order transverse modes are inadvertently permitted in addition to the intended changes in lateral-mode structure, we have shown that there is no effect on the proper detection of the coherence state for either a perfectly aligned receiver or for a translational offset in either the lateral or the transverse direction. The presence of higher-order transverse modes affects the intended measurement if there is a rotational misalignment; this effect was found to be negligible at reasonable tilt angles ( $10^\circ$ ), as long as the weights of the lateral modes are still kept equal.

We have examined the effects of misalignments only for cases in which the lateral-mode structure is 50% of the energy in each of the lowest two lateral modes. This particular condition was examined because it is the optimum place to operate a spatial-coherence-modulated link, as was demonstrated in Ref. 5. The link is surprisingly robust, particularly under rotational as well as transverse offsets, where the transverse direction is defined as the direction perpendicular to the direction in which modes are modulated. The link is also fairly insensitive to spurious higher-order spatial modes in the plane perpendicular to that under modulation. Because of these insensitivities and the high speeds that are attainable, spatial-coherence modulation appears to be an attractive method for increasing the information-carrying capacity of optical free-space communication systems.

This study was supported in part by National Science Foundation grant ECS-9108425.

## References

1. J. L. Brooks, R. H. Wentworth, R. C. Youngquist, M. Tur, B. Y. Kim, and H. J. Shaw, "Coherence multiplexing of fiber-optic interferometric sensors," *J. Lightwave Technol.* **LT-3**, 1062–1071 (1985).
2. K. W. Chu and F. M. Dickey, "Optical coherence multiplexing for interprocessor communications," *Opt. Eng.* **30**, 337–344 (1991).
3. J.-P. Goedgebuer and A. Hamel, "Coherence multiplexing using a parallel array of electrooptic modulators and multimode semiconductor lasers," *IEEE J. Quantum Electron.* **QE-23**, 2224–2236 (1987).
4. J.-P. Goedgebuer, A. Hamel, H. Porte, and N. Butterlin, "Analysis of optical crosstalk in coherence multiplexed systems employing a short coherence laser diode with arbitrary power spectrum," *IEEE J. Quantum Electron.* **26**, 1217–1226 (1990).
5. B. L. Anderson and L. J. Pelz, "Spatial coherence modulation for free-space communication," *Appl. Opt.* **34**, 7443–7450 (1995).
6. P. Spano, "Connection between spatial coherence and modal structure in optical fibers and semiconductor lasers," *Opt. Commun.* **33**, 265–270 (1980).
7. L. J. Pelz and B. L. Anderson, "Practical use of the spatial coherence function for determining laser transverse mode structure," *Opt. Eng.* **34**, 3323–3328 (1995).
8. M. Born and E. Wolf, *Principles of Optics*, 6th ed. (Pergamon, New York, 1980), Chap. 10, pp. 505–507.
9. B. L. Anderson and P. L. Fuhr, "Twin-fiber interferometric method for measuring spatial coherence," *Opt. Eng.* **32**, 926–932 (1993).